Imaging Methods for MEG/EEG Inverse Problem

Odyssee Laboratory ENPC - ENS Ulm - INRIA France

Geoffray Adde
Email: adde@certis.enpc.fr

Maureen Clerc
Email: Maureen.Clerc@sophia.inria.fr

Renaud Keriven
Email: keriven@certis.enpc.fr

***Abstract*— Recovering electrical activity of the brain from MEG/EEG measurements is known as the MEEG inverse problem. It is an ill-posed problem in several senses. One is that there is further less data observed than data to recover. One way to address this issue is to search for regular solutions. We present here a framework for applying image processing filtering techniques to the MEEG inverse problem. Exprimentations are presented on synthetic dara and validation is carried out on one real MEG data set.**

I. Introduction

The MEG/EEG inverse problem of reconstructing electrical sources in human brain is an ill-posed and under-determined problem. There are many classes of methods for solving this problem, each one having its advantages and drawbacks. The most used one is the moving dipole[7]. Among the other ones, Imaging methods are sometimes addressed with a Bayesian stochastic framework [4]. Minimum norm solutions and Tikhonov regularization can also be seen as variational regularization methods for removing this undetermination. These methods tend to produce a well-know scaterring and blurring effect on the reconstructed sources. We propose a framework for applying more sophisticated regularization techniques arrising from image processing field.

II. Imaging Methods and Variational Priors

A. Imaging Methods

The most measurable part of the electrical activity of the brain is widely believed to arise from pyramidal cells lying at the surface of the cortex. Hence, the electrical sources to be reconstructed can be modeled as a dipolar current distribution defined all over the cortex and normal to it at each point. Solving the inverse problem (IP) is thus finding the intensity of this source which we denote s. We denote H the transfer matrix of the linear function mapping a given source value s to the corresponding MEG/EEG measurements m. Defining the followong notations:

- $J_{DATA}(s) = \|H.s - m\|^2$
- $J_{SMOOTH}(s)$ a non-negative (preferably convex) function of s penalizaing non smooth distributions.
- α a non negative smoothing parameter

The solution of the IP is given by:

$$s_{mix} = \underset{s}{argmin}\ J_{DATA}(s) + \alpha.J_{SMOOTH}(s) \qquad (1)$$

For instance, if $J_{SMOOTH}(s) = \frac{\|s\|^2}{2}$, we get the well-known Tikhonov regularization. There is an other way to constrain the inverse problem. Indeed, if we take a look at the minimum norm-solution, it can be written using the same J_{SMOOTH} but with a different minimization problem:

$$s_{cons} = \underset{s \in {J_{DATA}}^{-1}(\{0\})}{argmin} J_{SMOOTH}(s) \qquad (2)$$

This is a different approach because of the hard data constraint. it can seem naive because of the existence of noise in real measures, the under-determination of the IP lets a huge degree of freedom for finding solutions. We think that using this hard constraint does not affect the final solution. Moreover, minimizing Eq.(2) exempts from choosing any smoothing parameter α. This is one major difference between our approach and previous work in [2] and this new approach shows to be more efficient and precise on synthetic tests. It is obvious using Eq.(2) that the minimum norm can be generalized to any kind of energy. In the following, we compare differents energies arising from the image processing field.

B. Anisotropic Diffusion as a Prior

If one adopts the image processing point of view, regularizaton of the IP can be interpreted as the deletion of an undetermination noise. It is then very natural to use image filtering techniques for building J_{SMOOTH}. Many of these techniques are based upon Partial Differential Equations (PDEs) implementing different kinds of diffusion processes. Among all these techniques, we focus on the ones which can be derived in a functional minimization framework. More precisely, all the energies included in this study are of the form:

$$J_{SMOOTH}(u) = \int_{\Omega} \Phi(\|\nabla u\|) d\Omega \qquad (3)$$

Where u is a flat image and Ω its domain. Using Euler Lagrange equation of Eq.(3), we get the following minimization PDE.

$$\frac{\partial u}{\partial t} = \Phi''(\|\nabla u\|) u_{\xi\xi} + \frac{\Phi'(\|\nabla u\|)}{\|\nabla u\|} u_{\eta\eta} \qquad (4)$$

$u_{\xi\xi}$ is the second directionnal derivative of u with respect to the direction of ∇u ($\xi = \frac{\nabla u}{\|\nabla u\|}$) and $u_{\eta\eta}$ is the second directionnal derivative of u with respect to the direction η orthogonal to ∇u. Further reading about these formulae is found in [3]. By this rewriting, the diffusion process generated by running Eq.(4) is decomposed into two components: one along the isophot (curve of same intensity on the image)

direction and the other one perpendiculary to it. Here follow some classical Φ functions and their decomposition :

Author	$\Phi(s)$	$\Phi'(s)/s$	$\Phi''(s)$
$Tikhonov$	$\frac{s^2}{2}$	1	1
$Rudin$[11]	s	$\frac{1}{s}$	0
$Perona$[8]	$-\frac{k^2}{2}(e^{-(s/k)^2-1})$	$e^{-(s/k)^2}$	$\frac{(1-2\frac{s}{k}^2)}{e^{(s/k)^2}}$
$Aubert$[5]	$\sqrt{1+(s/k)^2}-1$	$\frac{1}{\sqrt{\frac{k^2+s^2}{k^2}}}k^{-2}$	$\frac{\lvert k\rvert}{(k^2+s^2)^{3/2}}$

Tikhonov regularization gives raise to an isotropic diffusion (in both directions diffusion strength equals 1). The corresponding minimization equation is the well-known heat equation $\frac{\partial u}{\partial t} = \Delta u$. Rudin's function induces anisotropic smoothing in a strong manner: it smoothes the image only along the isophot direction. It permits an excellent preservation of the edges of the image. The corresponding energy is, by definition, the total variation (TV) of the image. The last two functions present intermediate strategies, trying to combine Rudin's strategy near the edges and isotropic smoothing far from them. More information can be found about these approaches and similar ones in [3]

As is, all these regularization terms are defined for flat images. They must be adapted to an image defined over a 2D manifold embedded in 3D space, namely the cortex. We get passed through this by just mentioning that one shoudl consider a surface metric that we denote ∇_S instead of ∇ (more informations about implementing intrinsic gradient can be found for example in [13]). In the following we will focus on the J_{SMOOTH} of the form $J^i_{SMOOTH} = \int\limits_S \Phi_i(\|\nabla_S s\|)dS$ for $i \in \{1,2,3,4\}$, Φ_i is the i^{th} fonction of the previous table and S is the surface of the cortex.

III. Implementation

Concerning the forward EEG/MEG problem, we use the symmetric formulation of the Boudary Elements Method (B.E.M) [6]. We use a mixed P1(piecewise linear)/P0(piecewise constant) discretization for respectively the electric potential on each interface and its normal derivative[1]. The source distribution s are discretized in a P1 basis.

A. Discretization

In order to implement the Φ-cost functions without lost of precision we keep the initial disretization of the source distribution i.e P1. In the following we discribe a way of calculating J^i_{SMOOTH} and its discrete gradient.

We denote n_T,n_V the number of triangles and the number of vertices of the source mesh. The P1 basis is denoted $(\phi^S_i)_{i=1\ldots n_V}$ such that ϕ^S_i is piecewise linear, equals 1 at vertex i and 0 at all other vertices. In each triangle T_j not containing vertex i, $(\phi^S_i) = 0$ and in each triangle T_j containing vertex i, we define $\mathbf{a}^j_i$ such that $(\phi^S_i)(x) = \mathbf{a}^j_i.x$. Moreover we denote $\mathbf{1}_j$ the indicator function of triangle j.

$$\begin{aligned}\int\limits_S \Phi(\|\nabla_S s(x)\|)dS(x) &= \sum_{k=1}^{n_T}\int\limits_{T_k}\Phi(\|\sum_{i=1}^{n_V} s_i \sum_{j=1}^{n_T}\mathbf{a}^j_i\,\mathbf{1}_j(x)\|)dS(x)\\ &= \sum_{k=1}^{n_T}\int\limits_{T_k}\Phi(\|\sum_{i=1}^{n_V} s_i\,\mathbf{a}^k_i\|)dS(x)\\ &= \sum_{k=1}^{n_T}\Phi(\|\sum_{i=1}^{n_V} s_i\,\mathbf{a}^k_i\|)\,A_k\end{aligned}$$

Note that one way to define ∇_S is to project the 3D gradient onto S. But here, the gradient is already tangent to the triangulated surface. We denote Q the linear application mapping the values of the source defined over the vertices of S to its gradient defined over the triangles of S:

$$\begin{array}{ccccc} Q: & X & \longrightarrow & (\mathbb{R}^3)^{n_T} \\ & \begin{bmatrix} s_1 \\ \vdots \\ s_{n_V}\end{bmatrix} & \longmapsto & \begin{bmatrix} \sum\limits_{i=1}^{n_V} s_i\,\mathbf{a}^i_1 \\ \vdots \\ \sum\limits_{i=1}^{n_V} s_i\,\mathbf{a}^i_{n_T}\end{bmatrix}\end{array}$$

and for $p = (p_1, p_2, ..., p_{n_T}) \in (\mathbb{R}^3)^{n_T}$, we set

$$\|p\|_{(\Phi,A_i)} = \sum_{i=1}^{n_T}\Phi(|p_i|)A_i \quad and \quad [p]_i = p_i$$

where $|.|$ is the Euclidian norm on $\mathbb{R}^3$ so that we get:

$$\int\limits_S \Phi(\|\nabla_S s(x)\|)dS(x) = \|Qs\|_{(\Phi,A_i)}$$

Computing the gradient is straightforward and gives:

$$\nabla J_{SMOOTH}(x) = Q^t\begin{bmatrix}\frac{[Qx]_1}{|[Qx]_1|}\Phi'(|[Qx]_1|)A_1 \\ \vdots \\ \frac{[Qx]_{n_T}}{|[Qx]_{n_T}|}\Phi'(|[Qx]_{n_T}|)A_{n_T}\end{bmatrix} \quad (5)$$

B. Algorithms

Solving the minimization problem (2) was carried out by a projected gradient algorithm:

Algorithm 1 (Projected Gradient Algorithm):

1. initialize the source reconstruction with the minimum norm solution: $s = pinv(m)$
2. compute the gradient direction $\mathbf{g}$ using Eq.(5)
3. compute the projection $\mathbf{g}'$ of $\mathbf{g}$ onto the kernel of H.
4. update the reconstructed source $s = s - \alpha\mathbf{g}'$
5. check stopping criterion and go to 2 if necessary
6. end

Several strategies were tested for the determination of an optimal step size α: numerical methods for exact search (gold section)[9], closed form solution with truncated series

expansion. Finally for efficiency reasons, we used a fixed step algorithm, which gives similar results.

IV. Experimentation and Results

All the algorithms were coded in C++. We used exclusively realistic head models. These models were build from anatomical MRI for each subject. These MRI were segmented using Brainsuite (a free software from USC [12]) for scalp and skull. The brain (more precisely the grey matter-white matter interface) was segmented using Absolut (an internal software from Odyssee Lab [10]).

A. Synthetic Benchmark

This first set of tests is based on a realistic head model taken from an experimentation run at Lena MEG center at Hôpital de la Pitié Salpêtri‘ere, Paris. The setup was 180 MEG sensors and 61 EEG patches. The source mesh had 34792 vertices. Appart from this, the head model was build using 3 interfaces (air-scalp, scalp-skull, skull-brain (including CSF)) for 4 nested domains (air, scalp, skull, brain+CSF). Each of the interfaces meshes was made of 700 vertices. Before any run of the IP, pre-computation is needed. For our given geometry, computing the transfer matrix H using our symmetric BEM implementation took 12 hours running on a Xeon 2.4GHz processor under linux. Once this precomputation done, each minimum norm solution is obtain by a mere matrix vector product. All other methods reach acceptable results at 2000 iterations in 200 seconds on the same machine for the MEG case. Complexity of the algorithm being linear with respect to number of measurements, EEG computations are approximately 3 times faster. All the results shown below are obtained with 10000 iterations in approximatvely 1000 seconds. This is a synthetic test : MEG and EEG measurements corresponding to a given source configuration are computed and then recontructed using all regularization methods.
This test is subdivided in four parts:

- **deep**: a source patch going deeper and deeper (5 steps)
- **discrim**: two sources patches getting closer and closer (5 steps)
- **number**: 5 patches scattered over the cortex successively appearing (5 steps)
- **size**: a growing source patch (5 step)

Illustrations of these test patches are available at: http://cermics.enpc.fr/∼adde/MEEGbench.

At first glance, for the MEG benchmark (Fig. 1), the minimum solution seems to always give the less correlated reconstrcution whereas TV gives, most of the time, the best one. More generally gradient based regularization method seem to perform better than minimum norm. Inside this subcategory, isotropic smoothing, as expected, blurs the source patches. This drawback doesn’t affect the purely anisotropic TV smoothing. Hybrid approach doesn’t improve TV’s results, maybe because of a fast numerical scheme. But EEG benchmark (Fig. 2) results provide us with what we believe to be a better explanation of the poor performances of hybrid

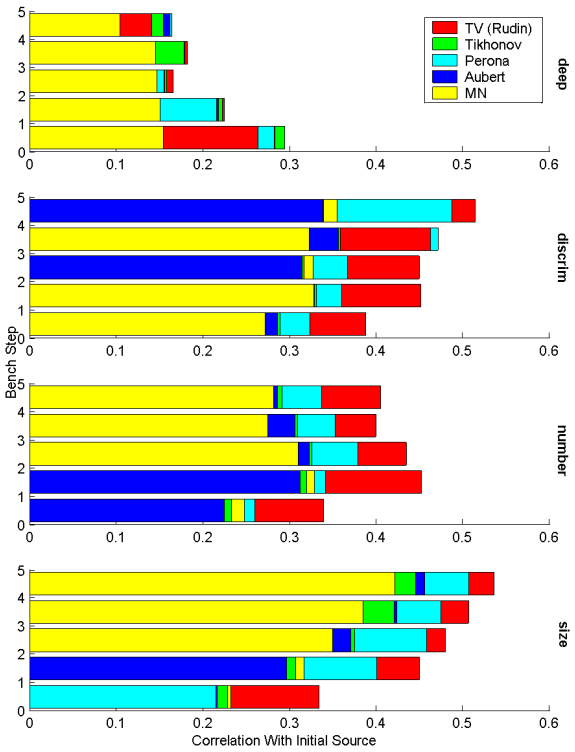

Fig. 1. MEG Synthetic Benchmark

smoothing methods. Indeed, for this benchmark all regularization methods show a performance breakdown comparing to the MEG benchmark. This phenomenon is due to the fewer available data and to the diffusion of the electric potential produced by the skull. This breakdown is significantly more important for hybrid smoothing methods and we do believe that these methods would benefit further than the other ones from an increase in the number of sensors. Numerical experimentations in this direction are in progress.

B. Real Data

In order to check the practical validity of the method, IP were run on a finger motor somatotopy experimentation. This set was given by Lena MEG center. A dipole fitting was performed using moving dipole method[7]. A good match between maxima of our reconstructions and fitting dipoles was found (Fig.3). This is only a visual clue because this goodness could not be quantified: : fitted dipoles are not constrained on the cortical surface. Our method is currently further compared to other distributed source methods on more real data sets.

V. Conclusion

We presented a framework that includes a class of image processing diffusion filters as regularization methods for the MEG/EEG inverse problem. In our approach no degree of freedom is left on the data driven part and the data constraint must

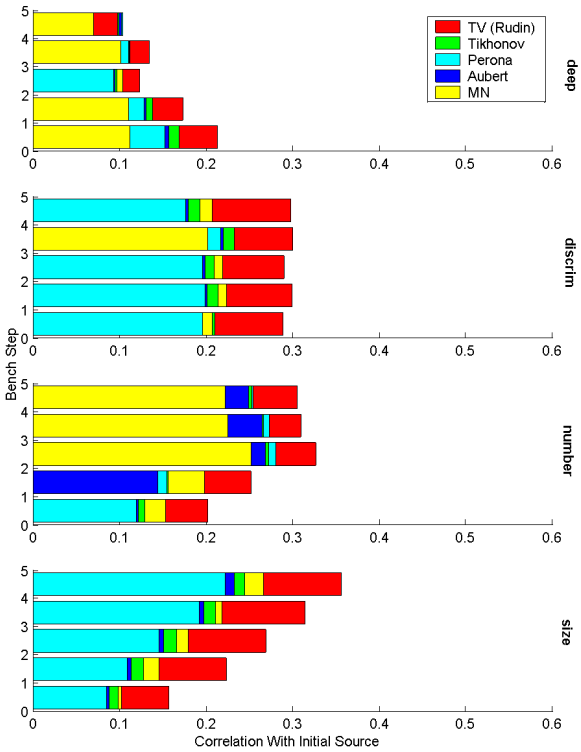

Fig. 2. EEG Synthetic Benchmark

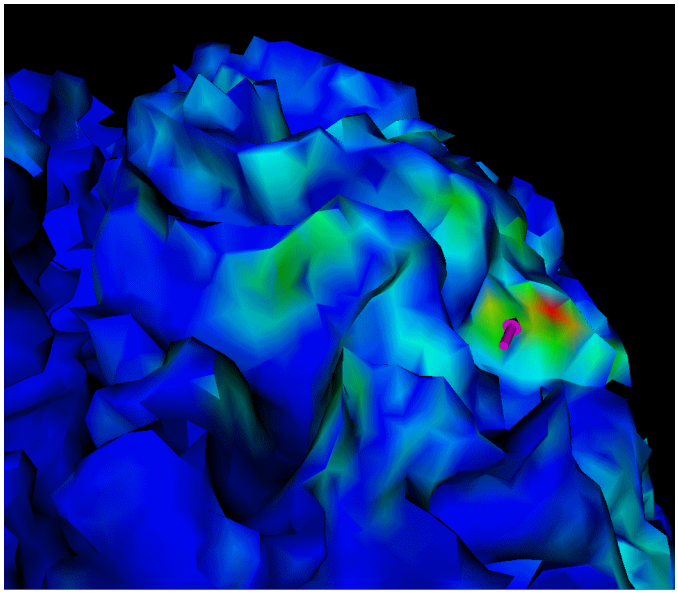

Fig. 3. Somatotopy Experimental Validation: TV imaging method compared to best moving dipole

be fullfilled. It permits to skip the selection of any smoothing parameter and gives faster and better convergence. Among all tested smoothing methods, Total Variation outperforms all the others including the most classic ones: minimum-norm and Tikhonov. Experimental validation is in progress and should permit to evaluate the practical utility of such techniques.

ACKNOWLEDGMENT

The authors would like to thank Anne-Lise Paradis (LPPA team CNRS, France) for her fruitful collaboration and for providing her experimental data. Our thanks also go to the Lena MEG center team for their technical support and for providing valuable input on understanding.

REFERENCES

[1] ADDE, G., CLERC, M., FAUGERAS, O., KERIVEN, R., KYBIC, J., AND PAPADOPOULO, T. Symmetric BEM formulation for the M/EEG forward problem. In *Information Processing in Medical Imaging* (July 2003), C. Taylor and J. A. Noble, Eds., vol. 2732 of *LNCS*, Springer, pp. 524–535.

[2] ADDE, G., CLERC, M., KERIVEN, R., AND KYBIC, J. Anatomy-based regularization for the inverse meeg problem. In *4th International Symposium on Noninvasive Functional Source Imaging within the human brain and heart* (Chieti, Sept. 2003).

[3] AUBERT, G., AND KORNPROBST, P. *Mathematical Problems in Image Processing: Partial Differential Equations and the Calculus of Variations*, vol. 147 of *Applied Mathematical Sciences*. Springer-Verlag, Jan. 2002.

[4] BAILLET, S., AND GARNERO, L. A bayesian approach to introducing anatomo-functional priors in the EEG/MEG inverse problem. *IEEE Transactions on Biomedical Engineering 44*, 5 (May 1997), 374–385.

[5] CHARBONNIER, P., AUBERT, G., BLANC-FRAUD, M., AND BARLAUD, M. Two deterministic half-quadratic regularization algorithms for computed imaging. In *Proceedings of the International Conference on Image Processing* (1994), vol. II, pp. 168–172.

[6] GESELOWITZ, D. B. On bioelectric potentials in an homogeneous volume conductor. *Biophysics Journal 7* (1967), 1–11.

[7] MOSHER, J. C., LEWIS, P. S., AND LEAHY, R. M. Multiple dipole modeling and localization from spatio-temporal MEG data. *IEEE Transactions on Biomedical Engineering 39*, 6 (1992), 541–553.

[8] PERONA, P., AND MALIK, J. Scale-space and edge detection using anisotropic diffusion. *IEEE Transactions on Pattern Analysis and Machine Intelligence 12*, 7 (July 1990), 629–639.

[9] POLAK, E. *Optimization : Algorithms and Consistent Approximations*, vol. 124 of *Applied Mathematical Sciences*. Springer-Verlag, 1997.

[10] PONS, J.-P., SGONNE, F., AND FAUGERAS, O. Extraction of head surface meshes from mri under topological constraints mri under topological constraints. In *unpublished* (2003).

[11] RUDIN, L., OSHER, S., AND FATEMI, E. Nonlinear total variation based noise removal algorithms. *Physica D 60* (1992), 259–268.

[12] SHATTUCK, D., AND LEAHY, R. Brainsuite: An automated cortical surface identification tool. *Medical Image Analysis 6*, 2 (June 2002), 129–142.

[13] SOCHEN, N., DERICHE, R., AND LOPEZ-PEREZ, L. Variational beltrami flows over manifolds. In *International Conference on Image Processing* (2003).